Berezinskii-Kosterlitz-Thouless transition effects on spin current: The normal-metal–insulating-ferromagnet junction case

R. J. C. Lopes,* A. R. Moura,† and W. A. Moura-Melo‡
Departamento de Física, Universidade Federal de Viçosa, 36570-900 Viçosa, Minas Gerais, Brazil

(Received 30 May 2020; revised 14 September 2020; accepted 27 October 2020; published 19 November 2020)

We investigate the temperature effects on the spin current through an interface between a normal metal and a quasi-two-dimensional ferromagnetic insulator. Conductive electrons are reflected at the interface absorbing or emitting magnons. The interaction process depends on the temperature, and we are interested in finding out how the transport of spin current is affected close to the Berezinskii-Kosterlitz-Thouless (BKT) transition. That is an important open question. While the thermodynamics of spin currents in the usual normal-metal–insulating-ferromagnet interfaces are known, the results of a BKT transition are still unknown. As it is well documented, the BKT transition is associated with the unbinding of vortex-antivortex pairs in two-dimensional models with an O(2) symmetry. In our work, the ferromagnet is a layered quasi-two-dimensional material, and in the limit of weak interplane coupling, a BKT transition is expected. Using the self-consistent harmonic approximation), we have obtained the BKT transition temperature (T_{BKT}) and the spin current as a function of the temperature. The spin current behavior at low temperatures is similar to those obtained from theoretical and experimental systems. At T_{BKT}, the spin current shows a discontinuous jump associated with vortex dissociation.

DOI: 10.1103/PhysRevB.102.184422

I. INTRODUCTION

Spintronics has emerged as an exciting field in the last years [1–3]. Instead of ordinary electric current, spintronics mainly deals with spin current, characterized by a net flux of spin. Spin currents propagate in both insulating or conducting materials, each one being magnetic or nonmagnetic, which diversify technological application. In nonmagnetic conductors, such as platinum, a spin current can be generated, for example, by conductive electrons moving in opposite directions according to their spin (the spin-up electron direction usually defines the spin current direction). This is the so-called pure spin current since there is no effective charge current. In a magnetic conductor, the charge current is also a spin current since the conductive electrons spins are naturally oriented. In insulators, the spin current is necessarily driven by spin waves, magnons in the quantum formalism, and it can be observed in ferromagnetic (FMI) [4–7], antiferromagnetic (AFI) [8–13] or even in paramagnetic (PMI) [13–17] insulators. Semiconductor materials have also played an important role in spintronics [18–21]. In particular, semiconductor-based spintronic devices have the potential of revolutionizing the technological industry, for a review see Ref. [20].

Spin currents can be generated and manipulated through the separation of up and down spins electrons in the charge current by means of spin-orbit coupling (the spin Hall effect, SHE) [22–26], temperature gradient (the spin Seebeck effect) [27,28] or by spin pumping using ferromagnetic resonance [5,29,30]. Conversely, one can detect spin current by converting it into charge current, which can be measured using conventional methods. In this case, usually, the process involves the inverse spin Hall effect [31–33], but it can also occur by the inverse Rashba-Edelstein effect [34] or spin-transfer torque [30,35,36]. Since magnon spin current has no energetic losses by Joule effect, magnetic insulators have often been used to generate and detect spin currents. Yttrium iron garnet, for example, is a widely used ferromagnetic insulator for spin current experiments [37].

A spin current injection at the interface between a normal metal (NM), also considered nonmagnetic, and a ferromagnetic insulator can occur in both directions. At equilibrium, spin current from the NM to FMI is equal in magnitude to the spin current in the opposite direction and, therefore, no spin current flows across the interface. One can create an effective spin current providing a nonequilibrium situation that favors the current in a specific direction. For example, in the spin-transfer torque process [30,38–40], a splitting chemical potential $\Delta\mu_e = \mu_\uparrow - \mu_\downarrow$ between up and down spin arises for the conduction electrons in the NM [6] close to the interface and, once free electrons are not able to penetrate into insulator, they reflect at the interface with inverted spins. In the case where $\Delta\mu > 0$, the creation of down spins is favored, and therefore spin-up electrons are annihilated when they reflect at the interface. Effectively, integer spin angular momentum is transmitted to the FMI, and the angular momentum conservation in the spin-flip scattering requires the appearance of a quantum of spin wave, a magnon, that bears spin-1. Whether the magnon has an up or down integer spin will depend on the ferromagnetic ground state orientation; however, an spin-up magnon has the same effect as a spin-down magnon moving in the opposite direction. In both cases,

*ricardo.lopes@ufv.br
†antoniormoura@ufv.br
‡winder@ufv.br

the spin current flows from the NM to the FMI. A similar process occurs when $\Delta\mu < 0$; however, in this case, the spin current direction is opposite to the latter one.

It is well-known that temperature has a main role in the spin current transmission. For example, there is no magnon excitation at zero temperature, and the spin conductivity vanishes. Besides, at zero temperature, all down electron states below $\mu_\downarrow$ are occupied, and it is impossible to occur the reflection of an up electron to a state with spin-down. Therefore, finite temperature effects are a necessary condition for spin current injection in the junction. In turn, FMI can present a topological phase transition at finite temperature, the so-called Berezinskii-Kosterlitz-Thouless (BKT) transition, which occurs in two-dimensional magnets bearing a continuous O(2) symmetry [41–45]. Instead of a spontaneous symmetry breaking, the BKT transition is associated with vortex-antivortex pairs unbinding. Below $T_{\rm BKT}$, the vortex-antivortex pairs are confined to stay together, leading to a quasi-long-range order. Vortex-antivortex unbinding occurs above $T_{\rm BKT}$, yielding to an exponential decay for the spin-spin correlation function, in place of the power-law decay for $T < T_{\rm BKT}$. Here, we model the FMI as composed of weakly coupled layers, which ensures the BKT transition [46–51].

In this work, we are interested in the effects of the BKT transition on the injection of spin current from a normal metal to a ferromagnetic insulator. We also determine the effects of the interplane interaction and the easy-plane anisotropy on the spin current injection. For determining the phase transition and its effects, we use the self-consistent harmonic approximation (SCHA). SCHA considers renormalized parameters that take into account higher orders in the operator expansion for the magnetic part. The magnon Green's function and the statistical average of spin operators are evaluated. As standard procedures, we apply linear response theory to find the spin current through the interface. The results show a discontinuous jump at $T_{\rm BKT}$ for spin current resistance. The low-temperature behavior agrees with that already reported in the literature.

II. THE MODEL

Following recent works [6,14], we divided the Hamiltonian into three parts: normal metal, magnetic insulator, and interaction interface term. The normal metal is considered as a free electron model with different chemical potentials $\mu_{\uparrow,\downarrow}$ for up and down electrons. In the second quantization formalism, the electronic Hamiltonian is written as $\hat{H}_e = \sum_{k\sigma}(\epsilon_k - \mu_\sigma)c^\dagger_{k\sigma}c_{k\sigma}$, where $c_{k\sigma}$ is the fermionic operator that annihilates an electron of momentum k and spin σ. At finite temperature, the electron propagation is given by the retarded Green's function $i\hbar G^{\rm ret}_{k\sigma}(t) = \theta(t)\langle\{c_{k\sigma}(t), c^\dagger_{k\sigma}(0)\}\rangle$ [52].

We considered a magnetic material composed of two-dimensional layers connected by an interplane coupling J^z. The Hamiltonian is given by

$$H_m = -J\sum_{\langle ij\rangle}\left(S^x_iS^x_j + S^y_iS^y_j + \lambda_{xy}S^z_iS^z_j\right) - J^z\sum_{\langle ij\rangle}\left(S^x_iS^x_j + S^y_iS^y_j + \lambda_zS^z_iS^z_j\right) - g\mu_BB_s\sum_i S^x_i, \quad (1)$$

where the first sum is performed over intraplane neighbors (coupling constant J), while the second sum is over interplane neighbors (coupling J^z), $0 \leqslant \lambda_{xy} < 1$ and $0 \leqslant \lambda_z \leqslant 1$ are easy plane anisotropies that favor the spins to align parallel to the XY plane to minimize the energy. As usual for many relevant materials [53–56], we consider a large interplane lattice parameter compared with intraplane sites, which lead us to $J^z \ll J$. Also, we will only consider the axial anisotropy λ_{xy} for the intraplane interactions. Finally, the Zeeman energy is associated with a uniform static magnetic field $\vec{B} = B_s\hat{x}$ and will be used to probe the spin of the magnon excitations.

There are many methods to obtain the spin propagator in the magnetic material. Takahashi *et al.* [6] used the ladder operators $S^\pm_i$ to define the magnon Green's function in an ordered FM model. It is also possible, for phases with broken symmetry, to represent the spin operators as bosonic operators using, for example, the Holstein-Primakoff (HP) formalism. However, HP bosons do not apply to disordered phases. Okamoto [14] adopted the Schwinger formalism to describe the spin current in the AF/FM in both ordered and disordered phases. In this case, the spin propagator is defined in terms of spinon (neutral collective modes with half-integer spin) operators. Although Schwinger formalism may be used to study the BKT transition, such a method is not the most appropriate, being necessary the addition of an auxiliary Abelian gauge field for the correct description of the BKT transition, as well shown in Refs. [57,58]. In order to obtain the BKT transition, we used the SCHA, described in Appendix A. Through the SCHA, we can write a quadratic Hamiltonian with renormalized parameters that take into account high order interactions. We also show that our calculations have a better agreement with experimental results than previous works.

The electrons of the magnetic insulator and normal metal interact by an *sd*-type exchange Hamiltonian [6,59] (an interaction between localized *d*-type electrons and conduction *s*-type electrons)

$$\hat{H}_{\rm sd} = J_{\rm sd}\sum_{qkk'}\left[S^z_q(c^\dagger_{k\uparrow}c_{k'\uparrow} - c^\dagger_{k\downarrow}c_{k'\downarrow}) + S^-_qc^\dagger_{k\uparrow}c_{k'\downarrow} + S^+_qc^\dagger_{k\downarrow}c_{k'\uparrow}\right], \quad (2)$$

where J_{sd} is the exchange coupling between conductor electrons and magnetic sites. The sum over the momenta q, k, and k' is made independently considering a rough interface and, therefore, the transverse component of momentum is not conserved. Here we adopted dimensionless spin operators with the $\hbar$ absorbed in the couplings J_{sd}, J, and J^z.

The spin current operator is defined as the time derivative $\hat{I}_s = (d/dt)\sum_{k\sigma}\hbar\sigma c^\dagger_{k\sigma}c_{k\sigma}$ and, using the Heisenberg equation of motion, we obtain

$$\hat{I}_s = iJ_{\rm sd}\sum_{qkk'}(S^-_qc^\dagger_{k\uparrow}c_{k'\downarrow} - S^+_qc^\dagger_{k\downarrow}c_{k'\uparrow}). \quad (3)$$

As one can note, when $\Delta\mu > 0$, spin-up electrons are destroyed while spin-down electrons are created in the spin-flip process. The same spin current operator can be obtained if we define the spin current in the FMI side of the interface as $\hat{I}_s = (d/dt)\sum_{q\sigma}\hbar\sigma a^\dagger_qa_q$, where a_q is the magnon annihilation operator.

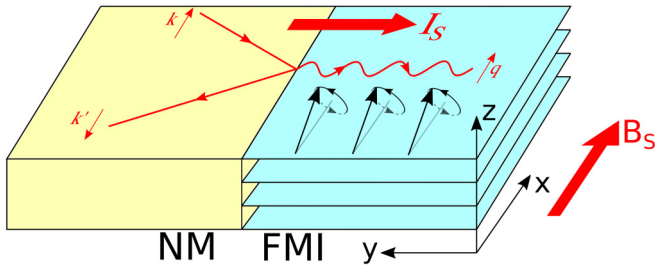

FIG. 1. Schematic example of a possible spin-flip process at the interface and the injection of magnons on the FMI side. An up spin electron with momentum k is reflected at the interface with down spin and momentum k' at the NM side. A magnon with up spin and momentum q is injected at the FMI side. B_s is a static magnetic field applied along the x direction, and I_s is the total spin current injected.

III. SPIN CURRENT

Using linear response theory [6], we obtain the expectation value of $\hat{I}_s$, defined in Eq. (3), as

$$I_s = \frac{1}{i\hbar}\int_{-\infty}^{\infty} dt\theta(t)\langle[\hat{I}_s(t), \hat{H}_{\rm sd}(0)]\rangle, \tag{4}$$

where the time evolution of the operators is obtained from the interaction picture. We define the operator $\imath\hbar\hat{U}(t) = \theta(t)[\hat{A}(t), \hat{A}^\dagger(0)]$, which provides the retarded Green's function

$$\imath\hbar U_{\rm ret}(t) = \theta(t)\langle[\hat{A}(t), \hat{A}^\dagger(0)]\rangle, \tag{5}$$

where $\hat{A}(t) = \sum_{qkk'} S_q^-(t)c_{k\uparrow}^\dagger(t)c_{k'\downarrow}(t)$. The $\hat{U}$ operator can be written as $\hat{U} = \hat{U}' + i\hat{U}''$, where $\hat{U}'$ gives the real part of $U_{\rm ret}$, while $\hat{U}''$ provides the imaginary one. It is easy to verify that $\hat{U}'(0) = 0$, and consequently $\mathrm{Re}[U_{\rm ret}(t)]$ vanishes for any t. To create a nonequilibrium situation that provides a spin current injection through the NM/FMI interface (Fig. 1), we introduce a spin-dependent chemical potential μ_σ in the NM part, where $\Delta\mu = \mu_\uparrow - \mu_\downarrow \neq 0$. After a straightforward procedure, the spin current is written as

$$I_s(\Delta\mu) = -2J_{\rm sd}^2 \mathrm{Im}U_{\rm ret}(\Delta\mu), \tag{6}$$

with the Fourier transform $U_{\rm ret}(\Delta\mu) = \int dt e^{\imath\Delta\mu t}U_{\rm ret}(t)$. From the Lehmann representation, we obtain $I_s(\Delta\mu) = 2\pi J_{\rm sd}^2\sum_{mn}P_{mn}\delta(K_m - K_n + \Delta\mu)$, with the transition probabilities given by

$$P_{mn} = \frac{(e^{-\beta K_m} - e^{-\beta K_n})}{e^{-\beta\Omega}}|\langle m|A|n\rangle|^2, \tag{7}$$

where K_m is the eigenvalue of the operator $\hat{K} = \sum_{k\sigma}(\epsilon_k - \mu_\sigma)$. Therefore, one notes that $I_s = 0$ in the limit of $\Delta\mu = 0$. As expected, if the up and spin-down electrons have the same chemical potential, then there is no effective spin inversion at the interface reflection, and $I_s = 0$.

As usual, since it is simpler to work with imaginary time $\tau = it$ than real time t, we adopted the Matsubara formalism to express the Green's function as

$$\hbar\mathcal{U}(\imath\Omega_m) = -\int_0^{\beta\hbar} d\tau e^{\imath\Omega_m\tau}\langle T_\tau\hat{A}(\tau)\hat{A}^\dagger(0)\rangle, \tag{8}$$

where $\Omega_m = 2\pi m/\beta\hbar$, $m \in \mathbb{Z}$, are the Matsubara frequencies and, T_τ is the imaginary time ordering operator. The retarded Green's function $U_{\rm ret}(\Delta\mu)$ is recovered adopting the analytic continuation $i\Omega_m \to \Delta\mu + i\epsilon$, where $\epsilon > 0$ is an infinitesimal parameter. Applying Wick's theorem, Eq. (8) is simplified to

$$\mathcal{U}(\imath\Omega_m) = -\hbar^2\sum_{qkk'}\int_0^{\beta\hbar} d\tau e^{i\Omega_m\tau}\mathcal{G}_{k\uparrow}(-\tau)\mathcal{G}_{k'\downarrow}(\tau)\mathcal{D}_q(-\tau). \tag{9}$$

The Matsubara Green's function of the electron is given by

$$\begin{aligned}\hbar\mathcal{G}_{k\sigma}(\tau) &= -\langle T_\tau c_{k\sigma}(\tau)c_{k\sigma}^\dagger(0)\rangle \\ &= \frac{1}{\beta}\sum_{\nu_n}\frac{e^{-i\nu_n\tau}}{i\hbar\nu_n - \xi_{k\sigma}} \\ &= e^{\xi_{k\sigma}\tau}[f(\xi_{k\sigma})\theta(\tau) - (1 - f(\xi_{k\sigma})\theta(-\tau))],\end{aligned} \tag{10}$$

where $\nu_n = (2n+1)\pi/\beta\hbar$, with $n \in \mathbb{Z}$, are the Matsubara frequencies for fermionic operators and, $\xi_{k\sigma} = \epsilon_k - \mu_\sigma$ is the electron energy relative to the chemical potential μ_σ. Here, we are considering a normal conducting state; however, a superconducting phase, for example, would be implemented by considering the phonon-electron interaction and adopting a coherent ground state in order to allow electrons to bind in Cooper pairs. The magnon Matsubara Green's function, defined by $\hbar\mathcal{D}_q(\tau) = -\langle T_\tau S_{-q}^-(\tau)S_q^+(0)\rangle$, was developed in Appendix B.

After replacing the Green's functions and evaluating the sum over the Matsubara frequencies, Eq. (9) yields

$$\begin{aligned}I_s = 2\pi J_{\rm sd}^2\sum_{qkk'}\Bigg[&\cosh^2\theta_q[n(\omega_q)(f(\xi_{k\uparrow}) - 1)f(\xi_{k'\downarrow})]\frac{\delta(-\xi_{k\uparrow} + \xi_{k'\downarrow} + \omega_q + \Delta\mu)}{n(-\xi_{k\uparrow} + \xi_{k'\downarrow} + \omega_q)} \\ &- \sinh^2\theta_q[(1 + n(\omega_q))(f(\xi_{k\uparrow}) - 1)f(\xi_{k'\downarrow})]\frac{\delta(-\xi_{k\uparrow} + \xi_{k'\downarrow} - \omega_q + \Delta\mu)}{n(-\xi_{k\uparrow} + \xi_{k'\downarrow} - \omega_q)}\Bigg],\end{aligned}$$

$$\begin{aligned}I_s = \frac{2\pi J_{\rm sd}^2}{n(-\Delta\mu)}\sum_{qk}&[\cosh^2\theta_q(n(\omega_q)(f(\xi_{k\uparrow}) - 1)f(\xi_{k\uparrow} - \omega_q - \Delta\mu)) + . \\ &- \sinh^2\theta_q((1 + n(\omega_q))(f(\xi_{k\uparrow}) - 1)f(\xi_{k\uparrow} + \omega_q - \Delta\mu))].\end{aligned} \tag{11}$$

Considering typical energy scales ($\epsilon_F \sim 10\,\text{eV}$, $\xi_k \lesssim 10^{-2}\,\text{eV}$ and $\hbar\omega_q$, μ_q, $\Delta\mu < \xi_k$), we can assume a continuous limit and integrate the Fermi-Dirac functions to obtain

$$\sum_k (f(\xi_{k\uparrow}) - 1) f(\xi_{k\uparrow} \pm \omega_q - \Delta\mu) \simeq \frac{V}{4}\left(\frac{2m_e}{\beta\pi\hbar^2}\right)^{3/2} \times \text{Li}_{1/2}(-e^{\beta\delta_\pm}), \tag{12}$$

where V is the NM volume, m_e is the electron mass, $\delta_\pm = \epsilon_F - (-3\Delta\mu \pm \hbar\omega_q)/2$ and $\text{Li}_s(x)$ is the polylogarithm (also known as Jonquière's function) of order s. Moreover, finally replacing the result from Eq. (12) in Eq. (11), we obtain the final expression for the spin current:

$$I_s = \frac{g_s T^{3/2}}{n(-\Delta\mu)} \sum_q [\cosh^2(\theta_q) n(\hbar\omega_q) \text{Li}_{1/2}(-e^{\beta\delta_-}) + \sinh^2(\theta_q)(1 + n(\hbar\omega_q)) \text{Li}_{1/2}(-e^{\beta\delta_+})], \tag{13}$$

in which we defined the constant,

$$g_s = \frac{V}{4}\left(\frac{2m_e k_B}{\pi\hbar^2}\right)^{3/2} (2\pi J_{sd}^2).$$

It is important to note that for high temperatures ($T > T_{\text{BKT}}$), the result should be interpreted with care. The SCHA method provides reliable results for temperatures $T < T_{\text{BKT}}$. However, above the BKT temperature, the self-consistent parameters vanish as well as the energy $\hbar\omega_q$ for all momentum. As a consequence, the spin current defined by Eq. (13) provides an infinite spin current for temperatures above the BKT transition. A detailed analysis reveals that the problem arises in the Green's function of the a operators. Indeed, since $\omega_q \to 0$ in the BKT transition, the a_q and $a_q^\dagger$ operators do not present time evolution, and any spin operator should be time independent. In particular, $S_q^-(t) = S_q^-(0)$ and the magnon Green's function $\hbar D_q^{\text{ret}}(t) = (-i\hbar)^{-1}\theta(t)\langle[S_q^-, S_q^+]\rangle = 2(-i\hbar)^{-1}\theta(t)\langle S_q^z\rangle = 0$ because H_q^ϕ tends to zero when $T \to T_{\text{BKT}}$. Therefore, at the transition temperature, we expect there will be no magnon propagation, and the spin current abruptly vanishes at $T = T_{\text{BKT}}$.

This different behavior, where the spin current vanishes after undergoing a BKT transition differs from that observed by Okamoto [14], which even after the system undergoes a phase transition, it still presents a finite propagation of the spin current. Actually, in Ref. [14] the transition from an FMI or AFI ordered system ($T < T_{\text{critical}}$) to a disordered PMI system ($T > T_{\text{critical}}$) is realized. This usual paramagnetic phase is generally composed of domains and the correlation length is finite (diverging only at the temperature where phase transition occurs). Regarding the BKT transition, for both $T < T_{\text{BKT}}$ and $T > T_{\text{BKT}}$, the system has no ordering at all [60]. It is disordered for any finite temperature. However, for $0 < T < T_{\text{BKT}}$, the correlation function follows a power law and the correlation length is infinite [41–43], that is, the system is critical at the whole temperature range, a feature which essentially differs our from that considered by Okamoto [14], where the system is critical only at the transition temperature. This regime is often called quasiordered and is characterized by the presence of bound vortices that contribute for disordering the system. These vortices also work like scattering potentials for magnons, as shown by Pereira *et al.* in Refs. [61,62]. For $T > T_{\text{BKT}}$, vortex-pair dissociation and proliferation completely disorders the system. In this paramagnetic regime, characterized by the excess of free vortices, the successive scattering experienced by the injected magnons in the system is enough to disorder the magnon propagation, breaking down any coherence in the spin current transport, consequently nullifying it.

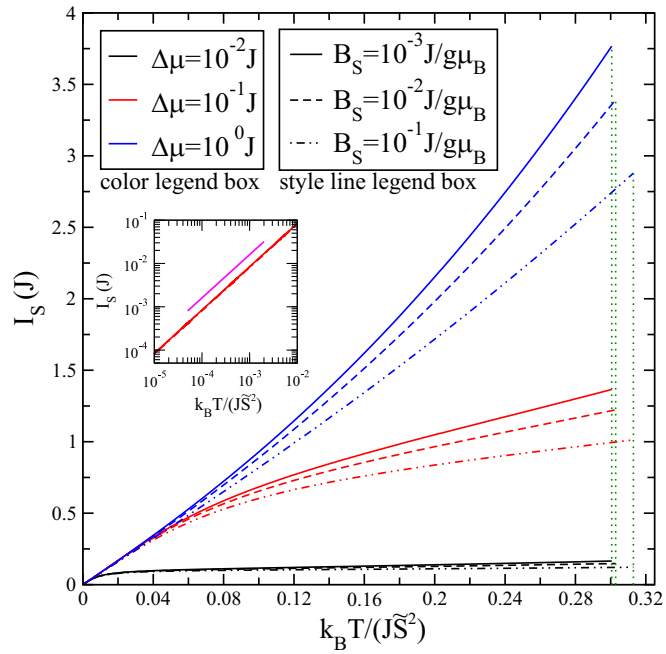

FIG. 2. Spin current vs T at different $\Delta\mu$ (represented by different colors), for a number of B_s (represented by different line styles). We have fixed $\eta = 10^{-3}$ and $\lambda_{XY} = 0.99$. The inset shows the linear behavior of I_s at a very low temperature. (The magenta line has a unity slope, and it only serves as a guide to the eyes). The curves above show the abruptly vanishing of spin current at BKT transition, as well as its reduction with the applied static field.

IV. RESULTS

For temperatures below T_{BKT}, the spin current presents a similar behavior when compared with references [6,7,14]. It increases with temperature and vanishes at $T = 0$. This comes about for thermal fluctuations increase the magnon population. At $T = 0$, there is no magnon excitation, so that the spin-flip process is prohibited, yielding that the spin current vanishes. Considering the classical magnon dispersion relation ($\omega_q \propto q^2$), it is easy to obtain $I_s \propto T^{3/2}$ from Eq. (13). This result is in accordance to previous theoretical [6] and experimental [7] results, even though our model is closer to the two-dimensional (2D) case. At very low temperatures, $T \to 0$, we also recover the theoretical result from [6], where $Is \propto T$.

In Fig. 2, we can also notice the expected reduction of the spin current with the increasing static magnetic field applied and the abruptly vanishing of the spin current at the BKT transition, as previously discussed. This behavior could be used as both an indirect signature for BKT transition and on

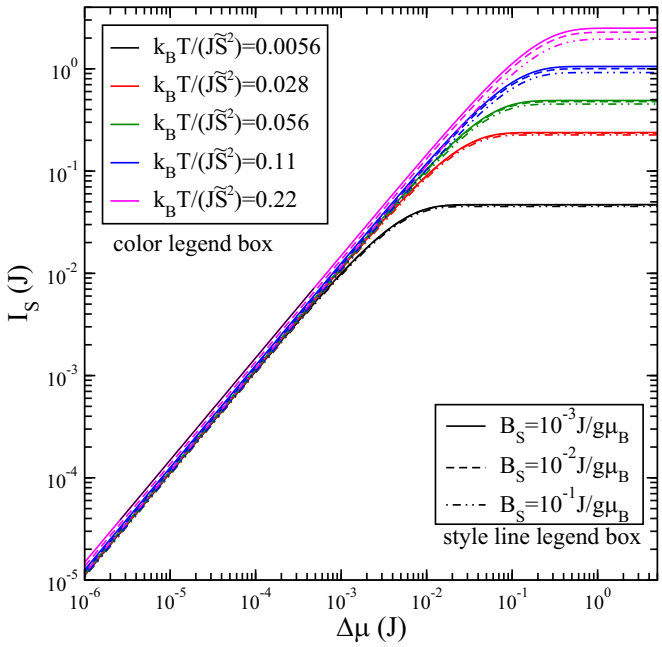

FIG. 3. Spin current vs the chemical potential for different temperatures and applied fields, showing the saturation of spin current for large $\Delta\mu$ values, in addition to the expected linear behavior for small $\Delta\mu$. We have used $\eta = 10^{-3}$ and $\lambda_{XY} = 0.99$.

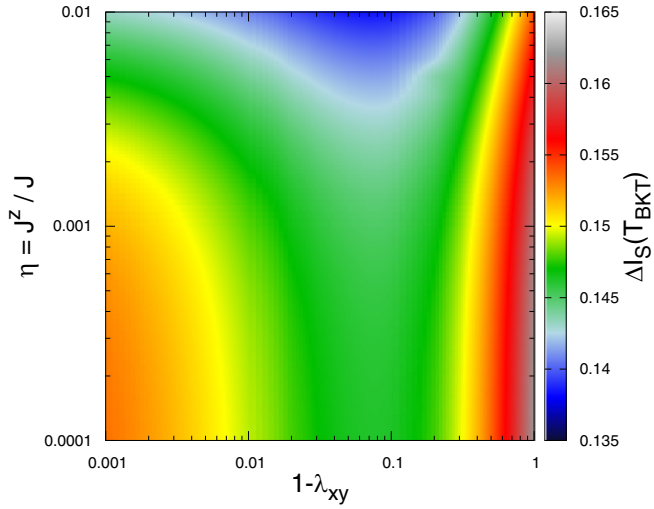

FIG. 4. Spin current jump, ΔI_s, at the T_{BKT}, with η and λ_{XY} varying. $\Delta\mu = 10^{-2}J$ and $g\mu_B B_s = 10^{-2}J$. Similar behavior occurs for different $\Delta\mu$ and B_s values. Lower η and λ_{XY} values, in addition to favor a BKT transition, lead to higher ΔI_s values, showing the importance of planar configurations to increase the magnon injection on the FMI.

pure spin current valve devices [63], which represent a crucial component to spintronics development. Finally, we can also see that, for small $\Delta\mu$ values, the injected spin current swiftly saturates with the temperature.

Another important result is how the spin current varies with $\Delta\mu$ at fixed temperatures. For low $\Delta\mu$ values, we recover the expected linear behavior [6,14], as shown in Fig. 3.

Besides the linear behavior, we also note that spin current injection saturates at larger $\Delta\mu$ values. This comes about for thermal fluctuations increases magnon population so that at a lower temperature, fewer magnons are created, which limits the possible spin-flip processes at the interface and consequently, the maximum spin current injected through FMI. In contrast, a higher (static) magnetic field decreases the magnon population, since the coupling between the magnetic field and the magnetic moments restricts their fluctuations.

According to Eq. (13), spin current jump $\Delta I_s = \lim_{T\to T^-_{\mathrm{BKT}}} I_s(T)$ not only depend on temperature, but also interaction parameters, chemical potential, and applied field. This nontrivial behavior is shown in Fig. 4. Despite the slight variation in ΔI_s, some expected behaviors can be observed. On the one hand, even for small interplane couplings, for fixed λ_{XY} values, increasing η leads to lower ΔI_s since, at higher η values, the system approaches a 3D isotropic Heisenberg model, which is disordered and presents no BKT transition. On the other hand, for fixed η values, lower λ_{XY} values (regime close to the XY model) yields higher ΔI_s values. In addition to BKT transition influence on the system, these two behaviors for η and λ_{XY}, also highlight the importance of planar spin configurations to increase the magnon injection on the FMI side.

V. CONCLUSIONS

In this work, we have studied the spin current injection through the interface between a normal metal and a quasi-2D ferromagnetic insulator. We have assumed a splitting chemical potential $\Delta\mu$ for the up and down electrons in the NM. These electrons reflect at the NM/FMI interface, and due to spin-flip processes, they emit (or absorb) magnons in the FMI side. Results for spin current injection in magnetic materials are known, but our work presents characteristics not yet observed in 3D systems. Here, we have considered a layered FMI whose layers are weakly coupled. Therefore, it is reasonable to take into account the BKT phase transition and its effects on the spin current.

We have used the SCHA method, which considers thermal renormalized parameters in order to include high order contributions, to express the magnon Green's function. The SCHA is a suitable formalism since the transition temperatures evaluated are in good agreement with experimental data. For potassium tetrafluorocuprate [53–55,64], for example, through the spin stiffness obtained from SCHA, the error between the BKT transition temperature obtained by us and the experimental result is less than 3%. Using linear response theory, we have obtained a spin current as a function of temperature, splitting chemical potential, static magnetic field, and coupling constants. Even though our model is closer to the 2D case, we have been able to retrieve the expected theoretical [6] and experimental [7] results for the spin current dependence on temperature ($I_s \propto T^{3/2}$), including the theoretical result [6] for very low temperatures ($I_s \propto T$). We also recovered the expected linear dependence [6,14] of spin current for small $\Delta\mu$ values ($I_s \propto \Delta\mu$).

However, when the BKT transition occurs, due to the vortices dissociation and proliferation, the spin stiffness suffers a discontinuity and the injected magnons are successively

scattered by the free vortices, disordering the magnon propagation and breaking down any coherence in the spin current transport, which induces an abrupt vanishing of the spin current. This result has not been described in the literature so far, and could be applied both to the indirect detection of a BKT transition and to application on pure spin current valve devices [63]. We have also verified the existence of an injection saturation for the spin current for large $\Delta\mu$ values. The value of saturation current varies with both temperature (higher temperature leads to higher saturation current), and static magnetic field applied (higher magnetic fields yields to lower saturation current).

ACKNOWLEDGMENTS

We thank A. R. Pereira, J. B. S. Mendes, E. F. Procópio, and N. T. Rodrigues for insightful discussions. We also acknowledge the financial support from FAPEMIG, CNPq, and CAPES (code-001) (Brazilian agencies).

APPENDIX A: SCHA

Conventional bosonic representations, like Schwinger [65–67], Holstein-Primakoff [68], and Dyson-Maleev [69–72] are not practical to treat BKT transition, we depart to adopt the SCHA [73–77]. The SCHA replaces the Hamiltonian given by Eq. (1) by a quadratic Hamiltonian with renormalized parameters that take into account higher-order contributions. Using the Villain representation [73], the ladder operators S^+ and S^- are represented by the φ and S^z operators as

$$S_i^+ = e^{i\varphi_i}\sqrt{S(S+1) - S_i^z\left(S_i^z+1\right)}, \tag{A1}$$

$$S_i^- = \sqrt{S(S+1) - S_i^z\left(S_i^z+1\right)}e^{-i\varphi}. \tag{A2}$$

Classically, φ and S^z fields obey Poisson brackets $\{\varphi_i, S_j^z\} = \delta_{ij}$ and, from quantum point of view, φ and S^z turn out to be canonically conjugate operators, *i.e.*$[\varphi_i, S_j^z] = i\delta_{ij}$. Considering a smooth spin field, we expanded the Hamiltonian (1) in powers of S_i^z and φ_i up to 2nd-order and, after a Fourier transform, we obtained

$$H = J\sum_q \left(H_q^\varphi \varphi_q\varphi_{-q} + H_q^z S_q^z S_{-q}^z\right), \tag{A3}$$

where we defined the coefficients $H_q^\varphi = 4\tilde{S}^2\rho(1-\gamma_q) + 2(J^z/J)\tilde{S}^2\rho^z(1-\gamma_q^z) + (\mu_B g B\tilde{S}/J)\zeta$ and $H_q^z = 4(1-\lambda_{xy}\gamma_q) + 2(J^z/J)(1-\lambda_z\gamma_q^z) + (\mu_B g B/(J\tilde{S}))$. Here, $\tilde{S}^2 = S(S+1)$, $\gamma_q = (\cos q_x + \cos q_y)/2$ and $\gamma_q^z = \cos q_z$ are structure factors for a quasi-2D square lattice. The intra- and interplane spin stiffness, ρ and ρ^z, respectively, and the ζ parameter are added to take into account higher order terms in the harmonic approximation, being determined by the Bogoliubov variational principle. Defining F as the Helmholtz free energy for the original Hamiltonian and F_0 as the free energy for the quadratic Hamiltonian then, ρ, ρ', and ζ should be chosen in order to satisfy the inequality $F \leqslant F_0 + \langle H - H_0\rangle$, where the mean value is evaluated using the harmonic Hamiltonian. Such a condition provides three self-consistent equations

$$\rho = \left(1 - \frac{\left\langle\left(S_i^z\right)^2\right\rangle}{\tilde{S}^2}\right)e^{-\frac{1}{2}\langle\Delta\varphi^2\rangle}, \tag{A4}$$

$$\rho^z = \left(1 - \frac{\left\langle\left(S_i^z\right)^2\right\rangle}{\tilde{S}^2}\right)e^{-\frac{1}{2}\langle\Delta\varphi_z^2\rangle}, \tag{A5}$$

$$\zeta = \left(1 - \frac{\left\langle\left(S_i^z\right)^2\right\rangle}{2\tilde{S}^2}\right)e^{-\frac{1}{2}\langle\varphi^2\rangle}. \tag{A6}$$

The statistical averages $\langle\Delta\varphi^2\rangle$ and $\langle\Delta\varphi_z^2\rangle$ are evaluated between the four intraplane neighbors and the two interplane neighbors, respectively. Expressing φ_q and S_q^z in terms of the new bosonic operator a_q, defined by

$$\varphi_q = \frac{1}{\sqrt{2}}\left(\frac{H_q^z}{H_q^\varphi}\right)^{1/4}(a_q^\dagger + a_{-q}), \tag{A7}$$

$$S_q^z = \frac{i}{\sqrt{2}}\left(\frac{H_q^\varphi}{H_q^z}\right)^{1/4}(a_q^\dagger - a_{-q}), \tag{A8}$$

we obtain the harmonic Hamiltonian

$$H_0 = \sum_q \hbar\omega_q\left(a_q^\dagger a_q + \frac{1}{2}\right), \tag{A9}$$

with the magnon energy $\hbar\omega_q = 2J\sqrt{H_q^\varphi H_q^z}$. Considering small both the axial anisotropy and the interplane interaction, a straightforward expansion to second order provides the characteristic quadratic magnon dispersion for FM in the absence of magnetic fields

$$\omega_q \approx \frac{2J\tilde{S}\sqrt{\rho(1-\lambda_{xy})}}{\hbar}\left(q_x^2 + q_y^2 + \kappa^2 q_z^2\right), \tag{A10}$$

where the z-axis anisotropy κ is defined as

$$\kappa = \sqrt{\frac{J^z\rho + J^z(1-\lambda_{xy})\rho^z}{2J\rho(1-\lambda_{xy})}}. \tag{A11}$$

By virtue of small interplane coupling, ω_q has a weak dependence with q_z and the magnon dispersion is almost constant along the z axis, parallel to NM/FMI interface. For $\lambda_{xy} = 0$ and $J^z = J$, $\kappa = 1$ and we recover the 3D isotropic dispersion $\omega_q = (2J\tilde{S}\sqrt{\rho}/\hbar)q^2$.

Using Eq. (A7), the following averages are determined in the thermodynamic limit:

$$\left\langle\left(S_i^z\right)^2\right\rangle = \frac{1}{2}\int\frac{d^3q}{(2\pi)^3}\sqrt{\frac{H_q^\varphi}{H_q^z}}\coth\left(\frac{\hbar\omega_q}{2T}\right), \tag{A12}$$

$$\left\langle\varphi_i^2\right\rangle = \frac{1}{2}\int\frac{d^3q}{(2\pi)^3}\sqrt{\frac{H_q^z}{H_q^\varphi}}\coth\left(\frac{\hbar\omega_q}{2T}\right), \tag{A13}$$

$$\langle\Delta\varphi^2\rangle = \int\frac{d^3q}{(2\pi)^3}(1-\gamma_q)\sqrt{\frac{H_q^z}{H_q^\varphi}}\coth\left(\frac{\hbar\omega_q}{2T}\right), \tag{A14}$$

$$\left\langle\Delta\varphi_z^2\right\rangle = \int\frac{d^3q}{(2\pi)^3}\left(1-\gamma_q^z\right)\sqrt{\frac{H_q^z}{H_q^\varphi}}\coth\left(\frac{\hbar\omega_q}{2T}\right). \tag{A15}$$

It is well known that the spin stiffness exhibits a universal jump at T_{BKT} associated with vortex proliferation

[41–43,75,76]. The spin stiffness vanishes for $T > T_{\rm BKT}$ while $\rho J\tilde{S}^2/T$ tends to $2/\pi$ when $T \to T_{\rm BKT}^-$. Therefore, φ should be split into two parts: $\varphi = \varphi_s + \varphi_v$, where φ_s describes the spin wave fluctuation, while φ_v is the vortex field. Unfortunately, the stiffness ρ obtained from SCHA takes into account only the spin wave contribution, neglecting any vortex effect. However, we can obtain the BKT temperature through the crossing between $\rho(T)$, obtained from the SCHA, and $2T/\pi J\tilde{S}^2$. In order to verify our equations, we determined the BKT temperature for potassium tetrafluorocuprate (K_2CuF_4), a well known layered ferromagnetic material with $S = 1/2$ [53–55,64]. Using $J = 23.86$ K, $J' = 0.016$ K and $J_a = 0.18$ K, the SCHA provides $T_{\rm BKT} = 5.35$ K, in accordance with the experimental measure $T_{\rm BKT} = 5.5$ K [54], and a better agreement than Irkhin [78] ($T_{\rm BKT} = 11.4$ K) and Sachs [53] ($T_{\rm BKT} = 7.9$ K).

APPENDIX B: THE MAGNON GREEN'S FUNCTION

The retarded magnon Green's function is defined by

$$\imath\hbar D_q^{\rm ret}(t) = \theta(t)\langle[S_q^+(t), S_{-q}^-(0)]\rangle_0, \tag{B1}$$

where we have considered mean values evaluated through the quadratic Hamiltonian from the SCHA. Using the Villain representation after the expansion of the ladder operators up to second order in φ and S^z, we obtain the mean value in momentum space

$$\begin{aligned}\langle[S_q^+(t), S_{-q}^-(0)]\rangle_0 &= \frac{1}{N}\sum_{\Delta r}\langle[S_i^+(t), S_{i+\Delta r}^-(0)]\rangle_0 e^{iq\Delta r}\\ &= \sinh^2\theta_q\langle[a_q^\dagger(t), a_q(0)]\rangle_0\\ &\quad + \cosh^2\theta_q\langle[a_q(t), a_q^\dagger(0)]\rangle_0\\ &= \langle[\mathfrak{a}_q(t), \mathfrak{a}_q^\dagger(0)]\rangle_0\ ,\end{aligned} \tag{B2}$$

where we define a new bosonic operator given by $\mathfrak{a}_q = \sinh\theta_q a_q^\dagger + \cosh\theta_q a_q$, with

$$\sinh\theta_q = \sqrt{J\left(\frac{H_q^\varphi + 4\tilde{S}^4 H_q^z}{4\tilde{S}^2\hbar\omega_q}\right) - \frac{1}{2}}, \tag{B3a}$$

$$\cosh\theta_q = \sqrt{J\left(\frac{H_q^\varphi + 4\tilde{S}^4 H_q^z}{4\tilde{S}^2\hbar\omega_q}\right) + \frac{1}{2}}. \tag{B3b}$$

The retarded magnon Green's function then takes the form:

$$\imath\hbar D_q^{\rm ret}(t) = \theta(t)\langle[\mathfrak{a}_q(t), \mathfrak{a}_q^\dagger(0)]\rangle_0\ , \tag{B4}$$

which is similar to that obtained from the Holstein-Primakoff formalism [68], which defines the ladder operators in terms of bosonic operators b_q as $S_q^+ = \sqrt{2S}b_q$ and $S_q^- = \sqrt{2S}b_q^\dagger$ (note that, in this case, the spin field is aligned along the z direction). By the definition of $D_q^{\rm ret}$, we interpret $\mathfrak{a}_q^\dagger$ as an operator that creates a magnon with spin along the z axis as well as $b_q^\dagger$ in Holstein-Primakoff representation. However, there is a difference in the spin orientation of the excited states obtained from our representation and the HP one. Since the ground state presents magnetization along the x direction, due to the static magnetic field, the lowest energy excitations should be long-wavelength spin waves with spin aligned along the magnetization direction. Therefore, a_q operators create magnons states with spin along the x direction, different from $\mathfrak{a}_q$ or b_q operators. Provided that the Hamiltonian given by Eq. (A9) is diagonalized by the a_q operators, we obtain $a_q(t) = e^{-i\omega_q t}a_q(0)$, whereas the states created by $\mathfrak{a}_q^\dagger$, which are not eigenstates of H, present a more complicated time evolution. As a consequence, the number operator $\mathfrak{a}^\dagger\mathfrak{a}$ does not commute with the Hamiltonian, as it is clear from the definition of $\mathfrak{a}$. Indeed, in the stationary state of the precession magnetization, the x component of the spin is conserved while the z component oscillates with a frequency defined by the energy eigenvalues. For that reason, the Green's function given by Eq. (B4) is composed of the linear combination of eigenstates of H_0 (at least for the case where the ladder operators are given by an expansion up to second order in φ and S^z). In the frequency space, the Green's function becomes

$$\hbar D_q^{\rm ret}(\omega) = \frac{\cosh^2\theta_q}{\omega - \omega_q + \imath\epsilon} - \frac{\sinh^2\theta_q}{\omega + \omega_q + \imath\epsilon}\ , \tag{B5}$$

in which, as usual, we introduced an infinitesimal factor $\imath\epsilon$ to ensure the convergence in the limit $t \to \infty$. The spectral function $R_q(\omega) = -2\,{\rm Im}\,D_q^{\rm ret}(\omega) = -2\pi\hbar^{-1}[\sinh^2\theta_q\delta(\omega+\omega_q) - \cosh^2\theta_q\delta(\omega-\omega_q)]$ provides two excitations, whose energies are given by $E = \pm\hbar\omega_q$. The negative energy excitation is associated with a magnon with inverse spin moving in the opposite direction, and therefore both modes contribute to the positive spin current.

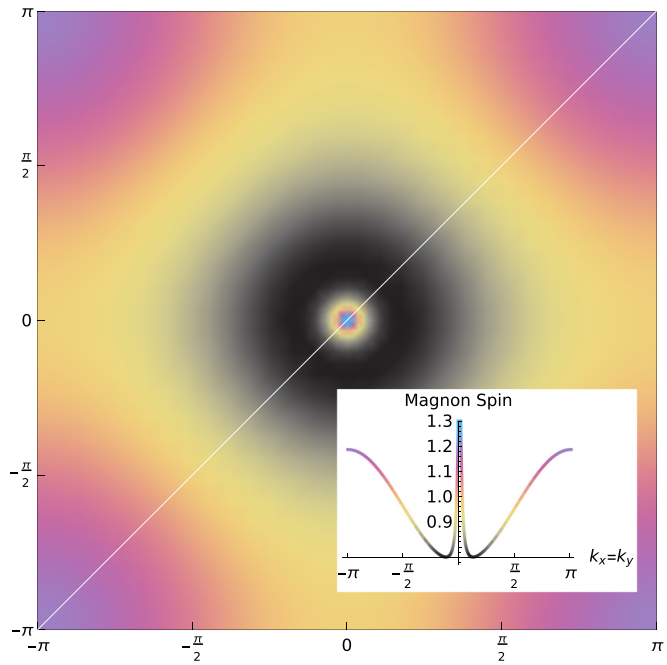

FIG. 5. The magnon spin in the Brillouin zone. Due to the adopted approximations, the spin is slightly larger than unity in some regions of the BZ but an average over the whole zone provides an according result. The inset shows the spin over the diagonal line.

TABLE I. The average spin $\langle S_m \rangle$ and the standard deviation σ of the excitation obtained from SCHA. The values are in accordance with the expected value of the magnon spin.

J^z/J	λ_{XY}	$g\mu_B B_s/J$	$\langle S_m \rangle$	σ
10^{-2}	0.90	10^{-1}	0.970	0.008
10^{-2}	0.90	10^{-2}	1.012	0.015
10^{-2}	0.99	10^{-1}	0.987	0.015
10^{-2}	0.99	10^{-2}	0.939	0.010
10^{-3}	0.90	10^{-1}	0.982	0.011
10^{-3}	0.90	10^{-2}	0.984	0.016
10^{-3}	0.99	10^{-1}	1.000	0.017
10^{-3}	0.99	10^{-2}	0.992	0.016

For finite temperature, it is useful to consider the Matsubara Green's function

$$\hbar \mathcal{D}_q(\omega_m) = \frac{\cosh^2 \theta_q}{\imath \omega_m - \omega_q} - \frac{\sinh^2 \theta_q}{\imath \omega_m + \omega_q}, \tag{B6}$$

with the bosonic frequencies $\omega_m = 2\pi m/\beta\hbar$, $m \in \mathbb{Z}$. After summing over the Matsubara frequencies, we have

$$\mathcal{D}_q(\tau) = \cosh^2 \theta_q \Upsilon_q(\tau) + \sinh^2 \theta_q \Upsilon_q(-\tau)\,, \tag{B7}$$

where

$$\hbar \Upsilon_q(\tau) = -\langle T_\tau a_q(\tau) a_q^\dagger(0) \rangle = -e^{-\omega_q \tau}[n_q + \theta(\tau)] \tag{B8}$$

represents the Matsubara Green's function for the a_q mode.

In order to probe the spin of the excitations described by the a operators, we evaluated the energy increase due to magnetic fields and associated it with the energy spin fluctuations. We can define the magnon spin $\langle S_m \rangle$ by the energy difference: $g\mu_B B_s \langle S_m \rangle = \langle \hbar\omega_q(B_s) - \hbar\omega_q(0) \rangle$, where the mean value is obtained over the first Brillouin zone. In Fig. 5, we show the result for $g\mu_B B_s = 0.01J$, $J^z = 10^{-3}J$, $\lambda_{XY} = 0.99$ and $S = 1/2$ (other combinations of J^z, λ_{XY} and B_s provide similar graphs). Since the propagators are evaluated considering a quadratic expansion in S^z and ϕ, the results are not exact; however, except for some regions of the first Brillouin zone, the spin value is only slightly larger than unity. The average over the Brillouin zone in Fig. 5 gives $\langle S_m \rangle = 0.992(16)$. For $S = 1/2$, we also found the average $\langle S_m \rangle$ and the standard deviation σ for many combinations of the interactions parameters and the static magnetic field B_s. As shown in Table I, the results are in agreement with the integer magnon spin.

[1] S. Wolf, D. Awschalom, R. Buhrman, J. Daughton, S. Von Molnar, M. Roukes, A. Y. Chtchelkanova, and D. Treger, Science **294**, 1488 (2001).

[2] I. Žutić, J. Fabian, and S. D. Sarma, Rev. Mod. Phys. **76**, 323 (2004).

[3] S. Bader and S. Parkin, Annu. Rev. Condens. Matter Phys. **1**, 71 (2010).

[4] Y. Tserkovnyak, A. Brataas, and G. E. W. Bauer, Phys. Rev. Lett. **88**, 117601 (2002).

[5] A. Azevedo, L. H. Vilela-Leão, R. L. Rodríguez-Suárez, A. F. Lacerda Santos, and S. M. Rezende, Phys. Rev. B **83**, 144402 (2011).

[6] S. Takahashi, E. Saitoh, and S. Maekawa, J. Phys.: Conf. Ser. **200**, 062030 (2010).

[7] S. Garzon, I. Žutić, and R. A. Webb, Phys. Rev. Lett. **94**, 176601 (2005).

[8] V. Baltz, A. Manchon, M. Tsoi, T. Moriyama, T. Ono, and Y. Tserkovnyak, Rev. Mod. Phys. **90**, 015005 (2018).

[9] J. B. S. Mendes, R. O. Cunha, O. Alves Santos, P. R. T. Ribeiro, F. L. A. Machado, R. L. Rodríguez-Suárez, A. Azevedo, and S. M. Rezende, Phys. Rev. B **89**, 140406(R) (2014).

[10] S. Takei, B. I. Halperin, A. Yacoby, and Y. Tserkovnyak, Phys. Rev. B **90**, 094408 (2014).

[11] S. M. Rezende, R. L. Rodríguez-Suárez, and A. Azevedo, Phys. Rev. B **93**, 054412 (2016).

[12] L. J. Cornelissen, K. J. H. Peters, G. E. W. Bauer, R. A. Duine, and B. J. van Wees, Phys. Rev. B **94**, 014412 (2016).

[13] W. Lin, K. Chen, S. Zhang, and C. L. Chien, Phys. Rev. Lett. **116**, 186601 (2016).

[14] S. Okamoto, Phys. Rev. B **93**, 064421 (2016).

[15] D. Wesenberg, T. Liu, D. Balzar, M. Wu, and B. L. Zink, Nat. Phys. **13**, 987 (2017).

[16] K. Oyanagi, S. Takahashi, L. J. Cornelissen, J. Shan, S. Daimon, T. Kikkawa, G. E. W. Bauer, B. J. van Wees, and E. Saitoh, Nat. Commun. **10**, 4740 (2019).

[17] V. S. U. A. Vargas and A. R. Moura, Phys. Rev. B **102**, 024412 (2020).

[18] A. Najmaie, R. D. R. Bhat, and J. E. Sipe, Phys. Rev. B **68**, 165348 (2003).

[19] Y. K. Kato, R. C. Myers, A. C. Gossard, and D. D. Awschalom, Phys. Rev. Lett. **93**, 176601 (2004).

[20] D. D. Awschalom and M. E. Flatté, Nat. Phys. **3**, 153 (2007).

[21] C. Brüne, A. Roth, E. Novik, M. König, H. Buhmann, E. Hankiewicz, W. Hanke, J. Sinova, and L. Molenkamp, Nat. Phys. **6**, 448 (2010).

[22] J. E. Hirsch, Phys. Rev. Lett. **83**, 1834 (1999).

[23] S. Zhang, Phys. Rev. Lett. **85**, 393 (2000).

[24] J. Sinova, S. O. Valenzuela, J. Wunderlich, C. H. Back, and T. Jungwirth, Rev. Mod. Phys. **87**, 1213 (2015).

[25] V. P. Amin and M. D. Stiles, Phys. Rev. B **94**, 104419 (2016).

[26] V. P. Amin and M. D. Stiles, Phys. Rev. B **94**, 104420 (2016).

[27] K. Uchida, S. Takahashi, K. Harii, J. Ieda, W. Koshibae, K. Ando, S. Maekawa, and E. Saitoh, Nature (London) **455**, 778 (2008).

[28] K. Uchida, J. Xiao, H. Adachi, J. Ohe, S. Takahashi, J. Ieda, T. Ota, Y. Kajiwara, H. Umezawa, H. Kawai, G. E. W. Bauer, S. Maekawa, and E. Saitoh, Nat. Mater. **9**, 894 (2010).

[29] A. Azevedo, L. Vilela Leao, R. Rodriguez-Suarez, A. Oliveira, and S. Rezende, J. Appl. Phys. **97**, 10C715 (2005).

[30] Y. Kajiwara, K. Harii, S. Takahashi, J. Ohe, K. Uchida, M. Mizuguchi, H. Umezawa, H. Kawai, K. Ando, K. Takanashi, S. Maekawa, and E. Saitoh, Nature (London) **464**, 262 (2010).

[31] E. Saitoh, M. Ueda, H. Miyajima, and G. Tatara, Appl. Phys. Lett. **88**, 182509 (2006).

[32] T. Kimura, Y. Otani, T. Sato, S. Takahashi, and S. Maekawa, Phys. Rev. Lett. **98**, 156601 (2007).
[33] S. O. Valenzuela and M. Tinkham, Nature (London) **442**, 176 (2006).
[34] K. Shen, G. Vignale, and R. Raimondi, Phys. Rev. Lett. **112**, 096601 (2014).
[35] M. D. Stiles and A. Zangwill, Phys. Rev. B **66**, 014407 (2002).
[36] D. C. Ralph and M. D. Stiles, J. Magn. Magn. Mater. **320**, 1190 (2008).
[37] P. Hyde, L. Bai, D. M. J. Kumar, B. W. Southern, C.-M. Hu, S. Y. Huang, B. F. Miao, and C. L. Chien, Phys. Rev. B **89**, 180404(R) (2014).
[38] J. Xiao and G. E. W. Bauer, Phys. Rev. Lett. **108**, 217204 (2012).
[39] A. Manchon, J. Železný, I. M. Miron, T. Jungwirth, J. Sinova, A. Thiaville, K. Garello, and P. Gambardella, Rev. Mod. Phys. **91**, 035004 (2019).
[40] M. Madami, S. Bonetti, G. Consolo, S. Tacchi, G. Carlotti, G. Gubbiotti, F. B. Mancoff, M. A. Yar, and J. Åkerman, Nat. Nanotechnol. **6**, 635 (2011).
[41] V. L. Berezinski, Zh. Eksp. Teor. Fiz. **59**, 907 (1971) [Sov. Phys. JETP **32**, 493 (1971)].
[42] V. L. Berezinski, Zh. Eksp. Teor. Fiz. **61**, 1144 (1972) [Sov. Phys. **34**, 610 (1972)].
[43] J. M. Kosterlitz and D. J. Thouless, J. Phys. C **6**, 1181 (1973).
[44] J. V. José, L. P. Kadanoff, S. Kirkpatrick, and D. R. Nelson, Phys. Rev. B **16**, 1217 (1977).
[45] R. Lopes and A. Moura, Phys. Lett. A **382**, 1492 (2018).
[46] M. E. Gouvea, F. G. Mertens, A. R. Bishop, and G. M. Wysin, J. Phys.: Condens. Matter **2**, 1853 (1990).
[47] A. S. T. Pires, A. R. Pereira, and M. E. Gouvêa, Phys. Rev. B **49**, 9663 (1994).
[48] A. R. Pereira, A. S. T. Pires, and M. E. Gouvea, Phys. Rev. B **51**, 16413 (1995).
[49] M. Ito, Prog. Theor. Phys. **66**, 1129 (1981).
[50] V. L. Berenzinski and A. Y. Blank, Zh. Eksp. Teor. Fiz **64**, 725 (1973) [Sov. Phys. JETP **37**, 369 (1973)].
[51] V. L. Pokrovski and G. V. Uimin, Zh. Eksp. Teor. Fiz 65, 1691 (1974) [Sov. Phys. JETP **38**, 847 (1974)].
[52] G. Rickayzen, *Green's Functions and Condensed Matter (Dover Books on Physics)* (Dover, New York, 2013).
[53] B. Sachs, T. O. Wehling, K. S. Novoselov, A. I. Lichtenstein, and M. I. Katsnelson, Phys. Rev. B **88**, 201402(R) (2013).
[54] K. Hirakawa, H. Yoshizawa, and K. Ubukoshi, J. Phys. Soc. Jpn. **51**, 2151 (1982).
[55] S. Hirata, N. Kurita, M. Yamada, and H. Tanaka, Phys. Rev. B **95**, 174406 (2017).
[56] J. B. Grant and A. K. McMahan, Phys. Rev. Lett. **66**, 488 (1991).
[57] A. S. T. Pires, L. S. Lima, and M. E. Gouvêa, J. Phys.: Condens. Matter **20**, 015208 (2007).
[58] N. Read and S. Sachdev, Phys. Rev. B **42**, 4568 (1990).
[59] J. Kondo, Solid State Phys. **23**, 183 (1970).
[60] N. D. Mermin and H. Wagner, Phys. Rev. Lett. **17**, 1133 (1966).
[61] A. Pereira, A. Pires, and M. Gouêa, Solid State Commun. **86**, 187 (1993).
[62] A. Pereira, A. Pires, and M. Gouvêa, Phys. Lett. A **176**, 279 (1993).
[63] J. Li, Y. Xu, M. Aldosary, C. Tang, Z. Lin, S. Zhang, R. Lake, and J. Shi, Nat. Commun. **7**, 10858 (2016).
[64] K. Hirakawa and H. Yoshizawa, J. Phys. Soc. Jpn. **47**, 368 (1979).
[65] J. Schwinger, *On Angular Momentum*, Technical Report No. NYO-3071, Harvard University, Nuclear Development Associates, United States, 1952.
[66] C. Lacroix, P. Mendels, and F. Mila, *Introduction to Frustrated Magnetism* (Springer, Berlin, 2011).
[67] A. Auerbach, *Interacting Electrons and Quantum Magnetism* (Springer-Verlag, New York, 1994).
[68] T. Holstein and H. Primakoff, Phys. Rev. **58**, 1098 (1940).
[69] F. J. Dyson, Phys. Rev. **102**, 1217 (1956).
[70] F. J. Dyson, Phys. Rev. **102**, 1230 (1956).
[71] S. V. Maleev, Zh. Eksp. Teor. Fiz **33**, 1010 (1958) [Sov. Phys. JETP **6**, 776 (1958)].
[72] S. Dembiński, Physica **30**, 1217 (1964).
[73] J. Villain, J. Phys. **35**, 27 (1974).
[74] A. S. T. Pires and M. E. Gouvêa, Phys. Rev. B **48**, 12698 (1993).
[75] A. Pires, Solid State Commun. **104**, 771 (1997).
[76] A. S. Pires and M. E. Gouvêa, Eur. Phys. J. B **44**, 169 (2005).
[77] A. Moura and R. Lopes, J. Magn. Magn. Mater. **472**, 1 (2019).
[78] V. Y. Irkhin and A. A. Katanin, Phys. Rev. B **60**, 2990 (1999).